Self-Affine Fractal Scaling in Fracture Surfaces Generated in Ethylene and Propylene Polymers and Copolymers

Fabrice Lapique,[1] Paul Meakin, Jens Feder, Torstein Jøssang

Department of Physics, University of Oslo, Box 1048, Oslo 0316, Norway

Received 31 August 2000; accepted 8 February 2002

ABSTRACT: The fracturing of four different polyolefin materials was studied with the objective of developing a better understanding of the relationships between the morphology of the semicrystalline polymers, the morphology of their fracture surfaces and their mechanical properties. This article is focussed on the quantitative description of the fractures surfaces. The surface structure can be described in terms of self-affine fractal models, and the Hurst exponent(s) and roughness measurements can be used to describe quantitatively the fracture surface topography. Fracture surfaces generated in homopolymers can be described by a single Hurst exponent, which differs for PE and PP. For copolymers with PE and PP matrices, the Hurst exponent measured on small-length scales was the same as that obtained for the matrix material, but a crossover to a second regime, with a higher Hurst exponent, was found at longer length scales. The crossover was related to the average distance between rubber particles for the PP/PE rubber phase specimen (PP-copo). The introduction of a second component seems to modify the crack propagation at long-length scales, but the propagation at shorter length scales remains unchanged. Environmental stress cracking experiments indicate that each regime can be related to brittle or ductile fracturing processes. © 2002 Wiley Periodicals, Inc. J Appl Polym Sci 86: 973–983, 2002

Key words: fracture; crack propagation; polymers; roughness; fractal geometry

INTRODUCTION

The main objective of the work described in this article was to study the relationships between the morphology of polymeric materials and the mechanical properties of products manufactured from them through the quantitative characterization of the fracture surface. The relationships between morphology and mechanical properties have been studied in a previous article.[1] The main focus of the present article is on the quantitative description of fracture surfaces. The fracture surface can be characterized by measuring the roughness and by studying its self-affine fractal geometry. Exploration of the relationships between the supermolecular structure, the fracture surface topography, and the fracture performance presents very exciting challenges, from both a basic research and an industrial point of view. If a link between the molecular structure and mechanical properties can be established, new concepts could be elaborated to design polymers with superior properties.

The materials that were studied are commercially important polyolefins (polyethylenes and polypropylenes). International standardized procedures (ISO standard) for industrial test procedures were followed in fracture experiments. The idea that the rough surfaces produced by the fracture of brittle materials have a self-affine fractal geometry[2,3] is now well established. The pioneering experimental work was carried out by Mandelbrot et al.[4] using steel. This work has been extended to a wide range of materials including other metals,[5–7] semiconductors,[5] cement-based materials,[8] ceramics and rocks,[5,9–13] polymers,[14] and natural anisotropic materials such as wood[15] and rocks.[10,12] In addition, the rough surfaces generated by a variety of simple computer models for material failure also appear to be self-affine fractals.[16] Some researchers have suggested that the Hurst exponent has a universal (independent of material and processing conditions) value,[17] but others have tried to relate the material dependent Hurst exponent to material properties such as the fracture energy.[9,18] Self-affinity and some mathematical tools to describe the statistically self-affine geometry of fracture surfaces are described later. Scanning electron microscopy (SEM) and optical microscopy, based on vertical scanning interferometry, were used to qualitatively and quantitatively characterize the fracture surfaces.

SAMPLES

Our study was focused on polyethylene- and polypropylene-based materials. Four different materials (see Table I), supplied by Borealis a/s (Rønningen, Norway) were chosen because of their relatively simple composition and their industrial interests: 2 polypro-

Correspondence to: Fabrice Lapique, SINTEF, P.B. 124 Blindern, N-0314 Oslo, Norway (Fabrice.Lapique@matek.sintef.no).

Journal of Applied Polymer Science, Vol. 86, 973–983 (2002)

TABLE I
Number-Average Molecular Weight M_n, Weight-Average Molecular Weight M_w, and Polydispersity of the Four Polymers

	M_n	M_w	Polydispersity
PP-homo	50,000	250,000	5
PP-copo	55,000	340,000	6.2
HDPE-homo	17,000	195,000	12
HDPE-copo	31,000	75,000	2.4

The values of M_n and M_w were determined by gel-permeation chromatography (GPC) at Borealis.

pylenes, referred to as PP-homo (a homopolymer) and PP-copo (a heterophasic propylene-ethylene copolymer), and two high-density polyethylenes referenced as HDPE-homo (a homopolymer) and HDPE-copo (a randomly distributed ethylene–hexene copolymer).

The specimens were prepared either by injection moulding (polypropylenes) or by hot pressing (polypropylenes and polyethylenes). In the injection molding cycle, the polymer was injected into the mold at a controlled speed (2–3-s injection time) and high temperature (200°C—well above the melting temperature). The mold temperature was 40°C, and the holding pressure needed to avoid sink marks (200 to 500 bars) was applied for 40 s. The specimen was then cooled down for 8 s (without applied pressure) and ejected. The total cycle time was about 60 s. Because of the high viscosity in the molten phase, the polyethylenes that were studied could not be injection molded. Consequently, a hot press was used. Pellets were placed between two metallic plates, which were then placed in the press. The hot pressing cycle started with compression–decompression subcycles during the melting of the pellets, to avoid air bubbles in the final sheets and to evaporate traces of residual solvent. The polymer plate was then compressed for 10 min at 180°C (5 min at low pressure and 5 min at high pressure). The specimens were then cooled at a rate of 15°C/min until a temperature of 40°C was reached. The hot press was also used to prepare the polypropylene samples, the only change being the compression temperature, which was 210°C.

All our specimens had the same shape: 10 mm wide and 80 mm long, with a thickness of 4 mm. To initiate fracture propagation in a specific location, the sheets were notched to a depth of 2 mm deep with a tip radius of 0.5 mm in one of the 4 × 80 mm faces.

TABLE II
Spherulites Size in the Center and along the Edge of the Fracture Surface

	Central part	Along the edge	Crystallinity
PP-homo (inj.)	60 μm	17 μm	49.4%
PP-copo (inj.)	30 μm	20 μm	43.8%
PP-copo (h.p.)	55 μm	45 μm	46.2%
HDPE-homo (h.p.)	32 μm	25 μm	57.5%
HDPE-copo (h.p.)	—	—	72.4%

Here, "inj." indicates that specimens were injection molded, whereas "h.p." indicates that specimens were hot pressed.

In our study, crystal sizes were measured with a crosspolarized light microscope. Thin slices (typically 10 μm) were microtomed and mounted between two glass plates using a rapid mounting media. Pictures were taken with a crosspolarized light microscope at different locations on the slices, to explore the influence of cooling rates and mechanical deformation rates during processing. The results are summarized in Table II.

FRACTURE EXPERIMENTS

A previous article[1] described in details the correlations between quantitative measures of the polymer structure and the mechanical properties of the final products. Fracture experiments were conducted at 23, 0, and −20°C to generate fracture surfaces under different experimental conditions for identical samples. Some of the results are summarized in Table III. It can be seen that for, all the samples but HDPE-copo, the fracture energy increases as the temperature is increased. The temperature and strain rate dependence of the fracture parameter J_c were also studied in the first part of this work.[1]

SELF-AFFINE FRACTAL ANALYSIS

Fracture surfaces have very complex structures that are difficult to describe in quantitative terms. In many studies, the surface topography is recorded and roughness averages (such as the average roughness Ra and the root-mean-square roughness rms) defined by the equations

TABLE III
Values of the Fracture Parameter J_c (kJ/m^2) at 23, 0, and −20°C Measured during Charpy Tests

	PP-homo (inj.)	PP-copo (inj.)	PP-copo (h.p.)	HDPE-homo (h.p.)	HDPE-copo (h.p.)
23°C	7.3 ± 0.6	20.5 ± 1.0	19.0 ± 1.0	18.6 ± 0.6pb	41.5 ± 1.5pb
0°C	2.5 ± 0.2	10.9 ± 0.3	11.1 ± 0.7	10.2 ± 0.3	46.0 ± 5.0pb
−20°C	2.7 ± 0.7	8.5 ± 1.5	8.1 ± 0.8	9.0 ± 0.6	43.2 ± 1.5pb

Here,"inj." indicates that specimens were injection molded, whereas "h.p." indicates that specimens were hot pressed. "pb" indicates that the samples were partially broken.

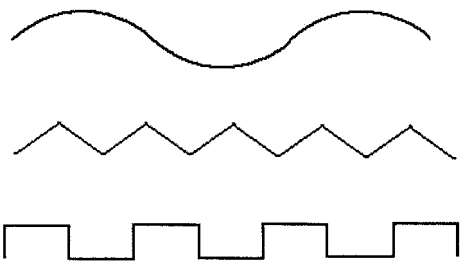

Figure 1 Surface profiles with the same Ra and rms roughness.

$$R_a = \frac{1}{n}\sum_{i=1}^{n} |Z_i - \bar{Z}| \tag{1}$$

and

$$R_{\text{rms}} = \sqrt{\frac{1}{n}\sum_{i=1}^{n} (Z_i - \bar{Z})^2} \tag{2}$$

are calculated, where N is the number of points, Z_i is the vertical coordinate of the ith point and $\bar{Z}$ is the mean value of the vertical coordinates. Measurement of the roughness does not provide a complete quantitative characterization of rough surfaces, because surfaces with the same R_a and rms roughness can have completely different appearances (see Fig. 1).

Therefore, the roughness determination should be combined with measurement of one or more shape parameters that tells us more about the structure of the surface. However, this approach has led to a plethora of morphometric parameters that are of little value in understanding either the structure or properties of rough surfaces. It has been shown that a wide range of fracture structure has a self-affine fractal geometry.[2,3,19–23] In general terms, a fractal is an object that has the same geometry on different length scales. The structure of most natural systems is complex and disorderly. Consequently, only statistical measures that characterize the structure are invariant to a change of length scale. In addition, the statistical characteristics of the structure are invariant to a change of length scale (expansion or contraction) over only a limited range of length scales. If the structure on a large scale is similar to the structure on a small scale when the length scale is changed isotropically, the object is said to exihibit self-similar scaling. But in natural processes (fracturing, for example) patterns often cannot be rescaled uniformly in all directions and still preserve (statistical) similarity. In general, each direction must be given an individual scaling factor. Patterns that require different rescaling factors in different directions are called self-affine. Self-affinity is an important symmetry that is related directly to many physical properties. If $h(x)$ is a self-affine function describing a profile of a fracture surface, it has the scaling properties

$$h(x) \equiv \lambda^{-H} h(\lambda x) \tag{3}$$

where $h(x) = 0$ at $x = 0$ and H is the Hurst exponent or roughness exponent ($0 \le H \le 1$). The symbol "≡" should interpreted as "statistically equivalent to." As shown on Figure 2, H is characteristic of the surface morphology. Similarly, if $h(X)$ is a self-affine fractal surface ($h(X) = h(x,y)$) is the height above or below a horizontal reference plane) then

$$h(x) \equiv \lambda^{-H} h(\lambda x) \tag{4}$$

where $h(X) = 0$ for $X = 0$. However, this is true only if the surface is homogeneous and isotropic in the lateral (X) directions. In general, the Hurst exponent obtained from analysis of the profiles may depend on the direction of the profile in the (x,y) plane and on the position at which the profiles are measured.

The measurement of the rms roughness and H can, therefore, give a precise quantitative description of important aspects of fracture surfaces. Many methods have been used to quantitatively describe the statistically self-affine geometry of the fracture surface. Surface width measurement has been used the most extensively.

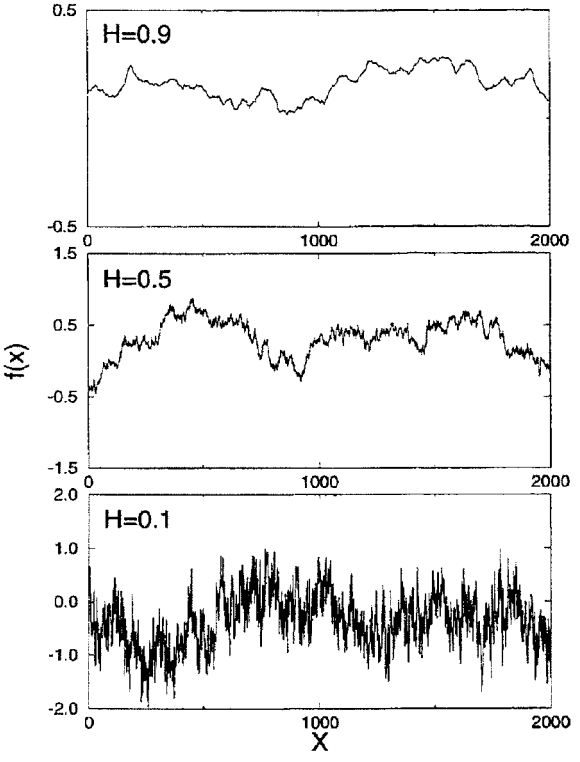

Figure 2 Surface profiles with different Hurst exponent H.

The bridge method and surface width measurements

In these methods, a profile of length L is divided into windows or bands of width Δ indexed by the lateral position of the first lateral point x_0 of the band. The standard deviation of the height ω and the difference δZ_{max} between the maximum and minimum height can be computed for the parts of the profile in all the possible bands obtained by varying the origin x_0 at fixed Δ, to obtain the averaged quantities $\langle \omega(\Delta) \rangle_{x_0}$ and $\langle \delta Z_{max}(\Delta) \rangle_{x_0}$. Bands with widths larger than $L/2$ are disregarded, because of insufficient independent sampling. For self-affine sets,[3] both quantities increase with increasing Δ, according to the power laws

$$\langle \omega(\Delta) \rangle_{x_0} \propto \Delta^H \quad \text{and} \quad \langle \delta Z_{max}(\Delta) \rangle_{x_0} \propto \Delta^H \tag{5}$$

where H is the Hurst exponent, or roughness exponent of the profile.[2,4–6] For a self-affine rough surface, the Hurst exponent H lies in the range [0:1]. The dependence of $\langle \omega(\Delta) \rangle$ on the window length Δ for a self-affine fractal indicates that the rms roughness has no fundamental meaning (the standard deviation of the height $\omega(\Delta)$ is equivalent to the rms roughness measured over a region of size Δ). I many systems $\langle \omega(\Delta) \rangle$ scales as $\langle \omega(\Delta) \rangle \propto \Delta^H$ over only a limited range of length scales $\Delta_{min} \leq \Delta \leq \Delta_{max}$ and $\langle \omega(\Delta) \rangle$ has a constant value for $\Delta \rangle \rangle \Delta_{max}$. Under these circumstances, the rms roughness can be used to characterize the geometry of fracture surfaces. However, care must be taken to ensure that rms roughness is measured over a sufficiently large window. Of course, the rms roughness can be measured at one or more Δ values, but the value used for Δ must be reported, and great care must be taken in comparing measurements from different sources.

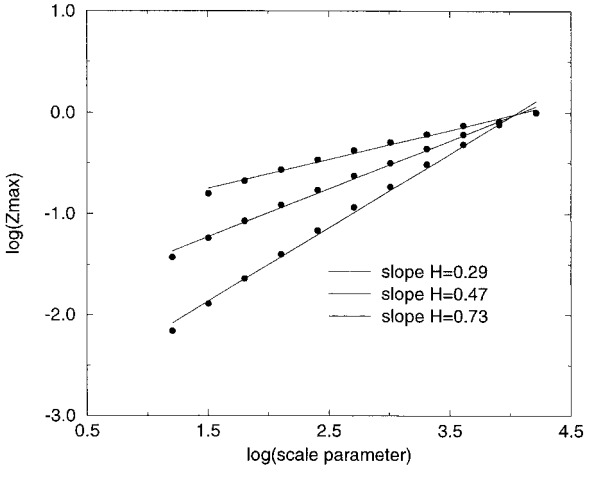

Figure 3 Determination of the Hurst exponent for three profiles generated with $H = .25$, $H = 0.50$, and $H = 0.80$, using the maximum surface width measurement approach. The scale parameter represents the quantity Δ, introduced in text.

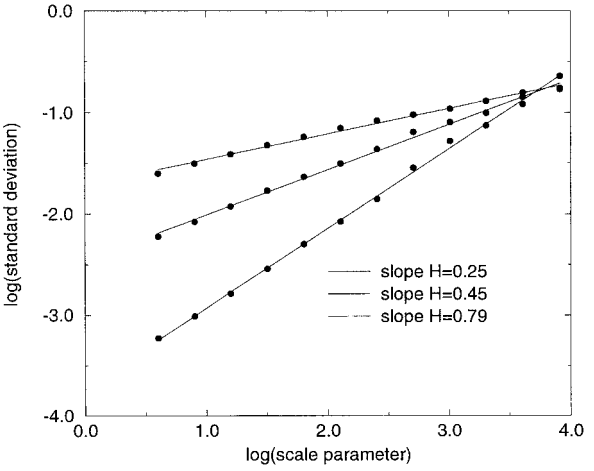

Figure 4 Determination of the Hurst exponent for the profiles analyzed in Figure 3, using the bridge method. The scale parameter represents the quantity Δ, introduced in text.

This method is very sensitive to possible tilting of the profile, which causes the effective value of the Hurst exponent to increase towards 1. Therefore, this approach can only be applied to horizontal profiles or profiles for which the "horizontal" direction is known, and the tilt can be removed. To avoid the effects of tilting, the bridge method[7,8] was used. It is very similar to the measurement of the standard deviation of the height ω, but the height is measured with respect to a reference line (the bridge) joining the first and last points of each window, *not the first and last points of the entire data set,* and the standard deviation $\langle \omega_{bridge} \rangle$ for the locally "detrended" profile is computed. For a self-affine set

$$\langle \omega_{bridge}(\Delta) \rangle_{x_0} \propto \Delta^H. \tag{6}$$

By using a reference line attached to the window, the influence of profile tilting is eliminated. To test the accuracy of the analysis methods discussed here, several tests have been performed on profiles generated (using fractional brownian motion) with roughness exponents of $H = 0.25$, 0.50, and 0.80. The results are presented in Figures 3–4.

Good agreement with the theoretical exponents was found. A variety of other methods have been used to measure the Hurst exponent of a self-affine profile. These include slit island analysis[4] (the analysis of horizontal cuts through the surface), Fourier analysis,[24] and wavelet analysis.[25–29]

RESULTS AND DISCUSSION

Fracture surfaces formed at 23°C are shown in Figures 5 to 8. A detailed and complete qualitative description of the fracture surfaces can be found in a previous articles[1] and only the main conclusions are repeated

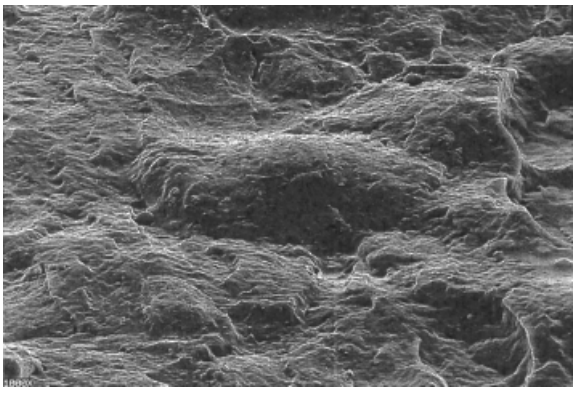

Figure 5 High magnification SEM picture of a PP-homo sample. The experiment was performed at 23°C. The size of the image is 290 × 225 μm.

here. The fracture surface of the PP-homo polypropylene was very regular, with a rounded hill and valley relief. No evidence of crazing or fibrillation could be observed, and the brittle fracture surface morphology did not seem to be temperature dependent.[1] Like the homoplymer, the two phases of PP copolymer fractured in a brittle manner. The fracture surfaces looked the same at both temperatures.[1] Small holes (black) and bumps (white) could be observed on the PP-copo fracture surface, due to the heterophasic nature of the polymer. The PP-copo material consists of a blend of polyethylene chains in a matrix of polypropylene, in which the two phases are not linked together. The boundary between polyethylene nodules and the polypropylene phase is a weak point in the copolymer structure. When a crack propagates, these nodules are pulled out from the matrix leaving holes on one of the fractures surfaces. Close inspection of the fracture surface indicated that the typical distance between nodules was in the 5–10 μm range.

The polyethylenes behaved in a totally different way. They are much more ductile materials that undergo crazing and fibrillation processes. Evidence of

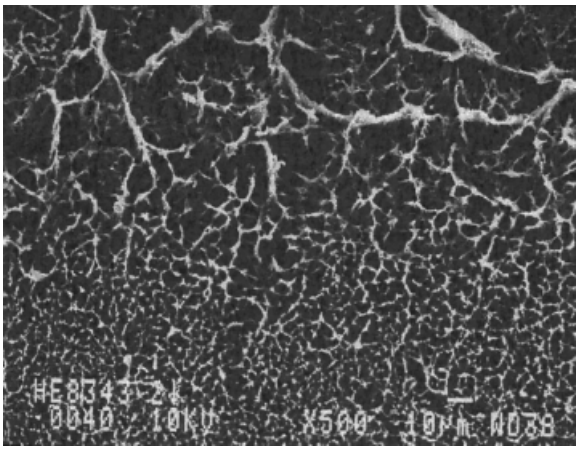

Figure 7 High magnification SEM picture of a HDPE-homo sample. The experiment was performed at 23°C.

crazing can be seen on the HDPE-homo fracture surface (see Fig. 7). During crack propagation, small craters, with very well-defined borders, were created on the fracture surface. The borders were made of crazed matter that was stretched in the direction perpendicular to the fracture plane. It can be seen that the crater pattern exists on a wide range of scales. The transition from coarse to fine structure is caused by irregular crack propagation, but it is remarkable that the coarse and fine structures look exactly the same. From a statistical point of view they are identical.

The fracture surface morphology of the high-density polyethylene copolymer (HDPE-copo) is also temperature independent[1] over the −20 to +23°C range. Like the homopolymer, the fibrillation process created cavities. The main difference is that relatively large sheet of highly deformed material were found in the fibrillation-induced network. Careful inspection of pictures at the highest magnification showed that the typical size of the cavities or craters was in the 5–10 μm range. This behavior also differs from that of the

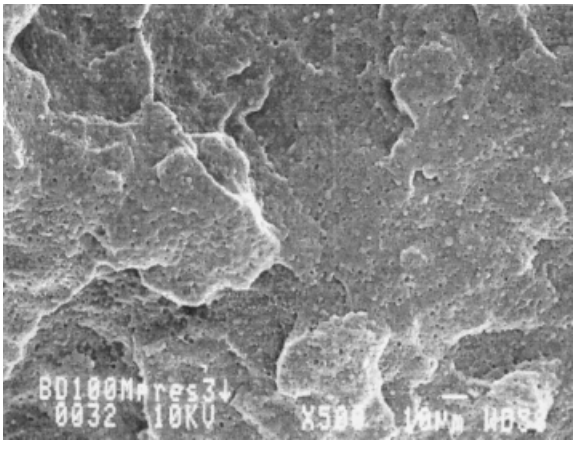

Figure 6 High magnification SEM picture of a PP-copo sample. The experiment was performed at 23°C.

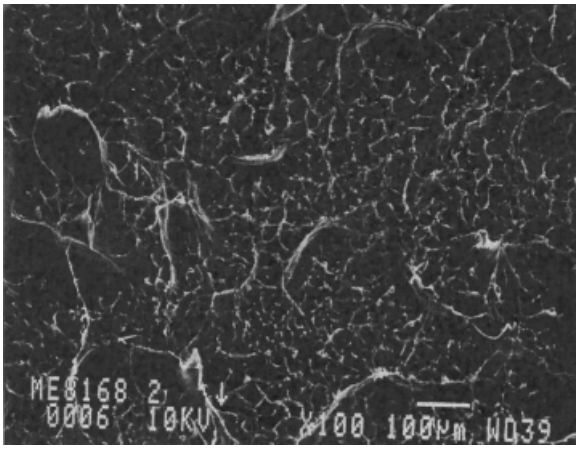

Figure 8 High magnification SEM picture of a HDPE-copo sample. The experiment was performed at 23°C.

homopolymer, for which it was impossible to identify characteristic features of any typical size.

Fracture surfaces from our five samples were studied quantitatively using a Wyko NT 2000 microscope based on vertical scanning interferometry. Pictures made with this microscope will be referred to as "Wyko pictures." The Wyko surface profiler system is a noncontact optical profiler that uses two technologies to measure a wide range of surface heights. The phase-shifting interferometry (PSI) mode allows us to measure smooth surfaces, while the vertical-scanning interferometry (VSI) mode allows us to measure rough surfaces and steps. The VSI mode is very well suited to study fracture surface topography. Vertical scanning interferometry is a newer technique than phase-shifting interferometry. The basic interferometric principles are similar in both techniques: light reflected from a reference mirror combines with light reflected from a sample to produce interference fringes, where the best contrast fringe occurs at best focus. However, in the VSI mode, the white-light source is not filtered, and the system measures the degree of fringe modulation, or coherence, instead of the phase of the interference fringes.

In vertical scanning interferometry, a white light beam passes through a microscope objective to the sample surface. A beam splitter reflects half of the incident beam to the reference surface. The beams, reflected from the sample and the reference surface, recombine at the beam splitter to form interference fringes. During the measurement, the reference arm containing the interferometric objective moves vertically to scan the surface at varying heights. A linearized piezoelectric transducer precisely controls the motion. Because white light has a short coherence length, interference fringes are present only over a very shallow depth for each focus position. Fringe contrast at a single sample point reaches a peak as the sample is translated through focus. The fringe contrast, or modulation, increases as the sample is translated into focus, then falls as it is translated past focus. The system scans through focus (starting above focus) at evenly spaced intervals as the camera captures frames of interference data. As the system scans downwards, an interference signal for each point on the surface is recorded. The system uses a series of advanced computer algorithms to demodulate the envelope of the fringe signal. Finally, the vertical position corresponding to the peak of the interference signal is extracted for each point on the surface. The vertical resolution in VSI mode is 3 nm. The lateral resolution is function of the magnification objective and the detector array size. Each magnification objective has its own optical resolution based on the magnification and numerical aperture of the objective. We have used magnifications having a lateral resolution of 0.7 and 0.16 μm.

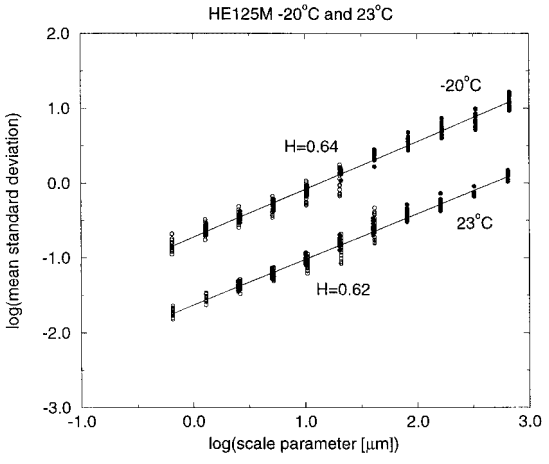

Figure 9 Evidence for the self-affine fractal scaling in the fracture surface of the PP homopolymer at 23°C and −20°C. The scale parameter represents the quantity Δ, introduced in text.

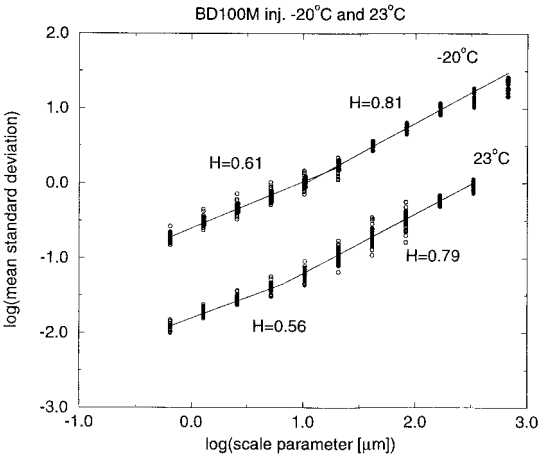

Figure 10 Evidence for the self-affine fractal scaling in the fracture surface of the injection molded PP copolymer at 23 and −20°C. The scale parameter represents the quantity Δ, introduced in text.

All the Wyko pictures capture very well the appearance of the fractures, and are very similar to the SEM pictures that were described in detail in a previous article.[1] The profiles taken in the direction perpendicular to the crack propagation were analyzed, using the numerical methods described later, and they were found to be self-affine. The results were similar for all the analysis methods, so only results obtained using the bridge method will be presented. To achieve a high resolution in our analysis, pictures with different sizes and spatial resolution were used. The $\omega_{\text{bridge}}(\Delta)$ curves obtained using the bridge method were collapsed onto a single curve to study the self-affine behavior of the profiles over more than 3 decades. The results are presented in Figures 9–13. For the sake of clarity, the curves obtained from fracture experiments conducted at 23°C are translated on the log–log plots. Otherwise, the points would have almost overlapped, because the fracture surface roughness did not vary

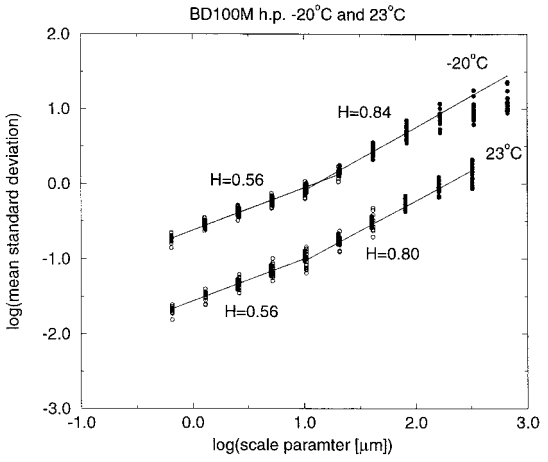

Figure 11 Evidence for the self-affine fractal scaling in the fracture surface of the hot pressed PP copolymer at 23 and −20°C. The scale parameter represents the quantity Δ, introduced in text.

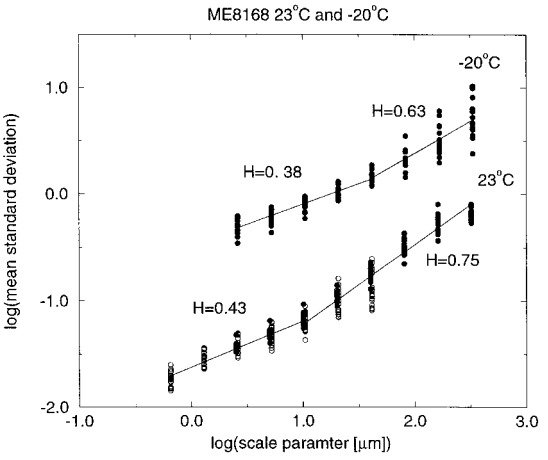

Figure 13 Evidence for the self-affine fractal scaling in the fracture surface of HDPE copolymer at 23 and −20°C. The scale parameter represents the quantity Δ, introduced in text.

significantly with temperature, even though the rms roughness is generally higher at 23°C (see Table IV).

Profiles were taken randomly at different positions on the fracture surface, and this is the origin of the vertical spread of the data points for a given length scale. The filled circles correspond to measurements performed on 1 × 0.5 mm images with a resolution of 0.7 μm (1428 points on each profile), whereas the unfilled circles come from the study of smaller images (46 × 60 μm) with a higher resolution, 0.16 μm (288 points on each profile). The data (usually 15 profiles from the large images and 15 from the small ones) collapse onto a single curve which supports the validity of our measurements.

The self-affine behavior of the fracture surfaces is confirmed, because the curves in Figures 9–13 can be fitted by straight lines over a wide range of length scales (almost 3 decades for homopolymers). This shows that the measurements of the Hurst exponent or roughness exponent can be used to differentiate surfaces with different topographies. All our fracture surfaces looked different, and their self-affine structure is characterized by a specific Hurst exponent or pair of Hurst exponents. It is striking that a single regime with a well-defined Hurst exponent was obtained for the PP or HDPE homopolymers over the entire length scales range that was accessible using our measurement techniques. However, copolymers are characterized by two self-affine regimes. We did not study enough samples to conclude that there is a direct correlation between the number of components and the number of regimes of self-affine behavior, but it would be worthwhile trying to expand these observations with a broader range of homopolymers and copolymers. However, it would be necessary to characterize the surface roughness over a very wide range of length scales to obtain convincing evidence for more than two self-affine scaling regimes. It can be argued that the copolymers behavior could also be fitted with a single smooth curve on a log–log scale. This interpretation would imply that the copolymer fracture surfaces are not self-affine. The data can be represented equally well using either two straight lines joined by a crossover or a smooth curve with no linear regimes. The model with two fractal regimes is more attractive, because the Hurst exponent obtained for the copolymers in the short length scale regime is the same as that for the homopolymer that forms the matrix. This suggests that the short-length scale fracture morphology is controlled by the matrix polymer and the long-length scale fracture geometry is controlled by the multicomponent polymer morphology.

It may be significant that for the PP-copo material, the transition between the two self-affine fractal regimes was found at a length scale close to 10 μm. This length is similar to the mean distance between poly-

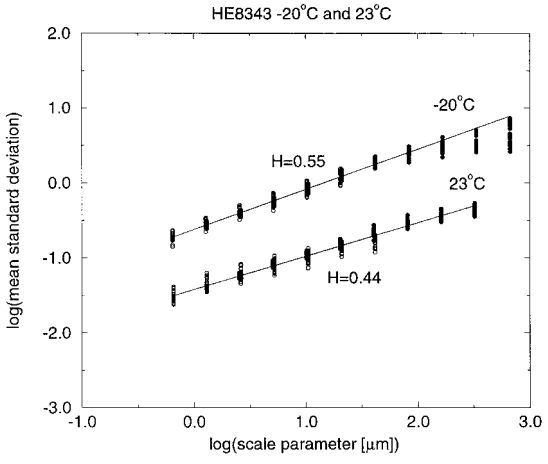

Figure 12 Evidence for the self-affine fractal scaling in the fracture surface of the HDPE homopolymer at 23 and −20°C. The scale parameter represents the quantity Δ, introduced in text.

TABLE IV
Roughness (rms) of Fracture Surfaces Generated at 23°C and −20°C

	PP-homo (inj.)	PP-copo (h.p.)	HDPE-homo (h.p.)	HDPE-copo (h.p.)
rms roughness (μm) 23°C	10.1	18.7	3.6	8.2
rms roughness (μm) −20°C	8.0	8.9	3.1	7.5

The roughness was measured for 1 × 0.5 mm images.

ethylene nodules, which was about 5–10 μm. This suggests that the small-length scale fracture morphology, with $H = 0.56$, can be correlated with the way in which the fracture propagates between consecutive nodules, whereas the other regime could characterize the propagation at longer length scales. This idea is supported by the observation that the role of these inclusions is to control the evolution and the propagation of the fracture. They are introduced into the matrix to arrest the propagation of the existing crazes and also to initiate the formation of new ones to consume as much as energy as possible in the fracture process. This is in good agreement with our self-affine analysis, which shows that the fracture surface can be characterized by two Hurst exponents, one for length scales smaller that approximately 10 μm and the other for longer length scales. This suggests that the fracture propagation is different in the essentially homogeneous material between the polyethylene inclusions than in the longer length scale "composite" structure. It would be very interesting to conduct the same study with PP-copo samples, with different concentrations of polyethylene nodules and determine if the mean distance separating two consecutive nodules and the length scale at which the crossover between the two self-affine fractal regimes takes place are correlated. The presence of the inclusions may be the reason why the fracture did not pass through the center of the spherulites (the nucleation point) as it did in the PP-homo case.[1] It appears that the crack does not propagate freely, as it did in the homopolymer, and that its course was constantly disturbed by the rubber particles.

A similar analysis was conducted for the HDPE-copo specimens. The transition between the two self-affine fractal regimes was found at a length scale close to 10 μm, which is similar to the mean distance between the lips of highly deformed material observed on the fracture surface (see Fig. 8).[1] These sheets of highly deformed material perturb and arrest the propagation of the existing crazes. Their creation consumes a lot of energy, and they act in the same manner as the PE nodules in the PP-copo material.

The homopolymers (PP-homo and HDPE-homo) have simple compositions (repetition of only one chemical entity), and can be considered to be homogeneous, even if the macromolecular structure is complex and inhomogeneous. This can explain why the self-affine structure can be described by only one Hurst exponent. But it is also very surprising that typical length scales characterizing the macromolecular structure such as the mean spherulite size do not appear as typical length scales in the study of the self-affinity of the surfaces. This is consistent with the conclusion that the spherulite size does not seem to have a direct influence on the mechanical properties of the final product. This idea was proposed in our previous article,[1] where it was shown that the fracture propagates independently of the spherulites arrangement. But it was also found that, in the PP-homo specimen, the fracture propagation was influenced by the lamellar orientation (the fracture passed through the spherulites following a radial path). In that case, the length characterizing the lamellar structure could be a relevant length scale in the fracture propagation process. To check this hypothesis, the dynamical range of our measurements must be extended. One way to do this would be to examine, at a high resolution, small areas of the fracture surfaces, using an atomic force microscope (or other high resolution device) and to use the same method to determine the Hurst exponent. If the fracture surface has a simple self-affine structure, the curves obtained should collapse with those obtained using the Wyko microscope and extend the dynamical range of the measurements.

Another interesting objective of this work was to determine if the self-affine analysis of the structure of the fracture surfaces could be used to differentiate materials with different compositions and the way in which they break (ductile or brittle behavior). Because our study was limited to four samples, we cannot provide general answers to these questions. Table V summarizes how the value of H depends on the material.

In the first regime, two values for the Hurst exponent were found depending on the matrix composition (polypropylene or polyethylene). The fracture surfaces of materials with a PP matrix have a Hurst

TABLE V
Hurst Exponents for All the Samples at 23°C

	H First regime	H Second regime
PP-homo	0.62 ± 0.02	—
PP-copo inj.	0.56 ± 0.03	0.79 ± 0.03
PP-copo h.p.	0.56 ± 0.03	0.80 ± 0.03
HDPE-homo	0.44 ± 0.02	—
HDPE-copo	0.43 ± 0.03	0.75 ± 0.03

exponent at small length scales close to 0.60, whereas the fracture surfaces of PE matrix materials have a lower Hurst exponent close to 0.45, over the same length scale range. We do not know why the PP samples have a higher H value than the PE specimens, but the difference found in our study suggests that the study of the self-affine structure of the fracture surfaces is able to distinguish between different materials, or at least materials that break in different ways. This work was concerned with only two polyolefin polymer families, it would be desirable to extend our study to other polymer families to evaluate the generality of the results.

The values of the Hurst exponents, measured at higher length scales, were quite similar for all materials that were studied, but they seem to be a little higher for the polypropylenes. The PP samples broke in a relatively brittle way, whereas the PE samples showed a more ductile behavior. It would have been very interesting to determine if the Hurst exponent could be related to the ductile or brittle mode of fracture. But it is very difficult to give an unambiguous answer based on the results that were obtained from surfaces generated by impact testing. To obtain more insight, another experiment was conducted to study fracture surfaces generated by environmental stress cracking. In this experiment, a thin rectangular bar of HDPE-copo material was bent and put in a solution of soap in water. A scratch was made on the specimen to initiate an environmental stress cracking process. After many hours in the solution, the specimen broke and the fracture surface was studied. It was surprising that the fracture surface was divided into two distinct zones. The first zone, generated in the early stages of the fractures propagation, has a morphology characteristic of brittle fracture, with a low roughness compared to the second zone of the fracture surface. In the second zone of the fracture surface, generated at a later stages, the fracture appeared to be more ductile, and there was evidence for a fibrillation process. The initial stress in the specimen was initially high. After some time in the aggressive solution the material was weakened and could not longer support the imposed stress. The crack propagated very rapidly, and the material behaved in a brittle manner. As the stress was released, the crack slowed down until the internal stress becomes too low for the brittle fracture process to continue. In this second regime, the specimen broke in a ductile manner. The conclusion is that the experiment leads to two different failure processes in two distinct regions of the fracture surface. This is important, because it allows us to measure the Hurst exponent for exactly the same material in each regime, and to establish a possible correlation between the fracture mechanism (ductile or brittle fracture) and the Hurst exponent.

The self-affine behavior of the fracture surface is illustrated in Figure 14 for the brittle and the ductile

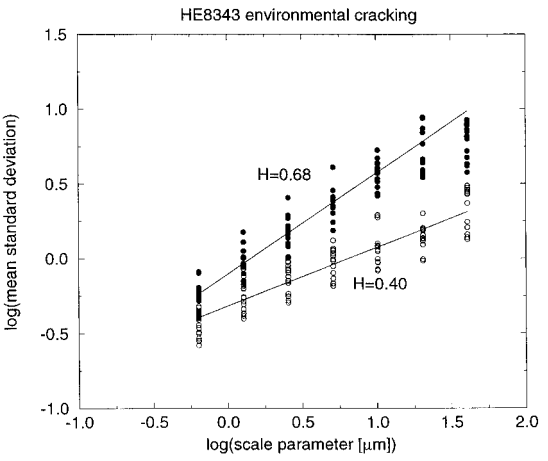

Figure 14 Study of the self-affine behavior of the fracture surface generated by environmental stress cracking. The unfilled circles correspond the initial brittle zone, whereas the filled ones represent the behavior of the final ductile zone of the fracture. The scale parameter represents the quantity Δ, introduced in text.

parts of the fracture. For each region, no evidence for a crossover was found, and the surface could be characterized by only one value of H. Hurst exponents of $H = 0.40$ for the brittle part and $H = 0.68$ for the ductile region were obtained. These values are similar to those measured for HDPE-homo and HDPE-copo specimens using impact testing (see Table V). This supports the idea that these two Hurst exponents are representative of the fracture surfaces of HDPE specimens and that the value of the Hurst exponent indicates the way in which the specimen failed (brittle or ductile). This means that products made from copolymers break in a more complicated way than products manufactured from homopolymers, and the two modes of failure are revealed by self-affine analysis of the fracture surfaces. All our conclusions are based on the study of a few materials, and a more systematic study should be carried out to assess the reliability and generality of these encouraging results obtained by using fractography and measuring the self-affinity of fracture surfaces to correlate the supermolecular structure with mechanical behavior.

Even if our conclusions are based on the study of only a few materials, it is interesting to discuss them with respect to existing experimental results and available models predictions. The change in the roughness exponent at smaller length scale measured in our experiments is reminiscent of the predictions from models of lines moving through randomly distributed obstacles. Models of lines moving through randomly distributed obstacles[30–32] have been used to simulate the propagation of cracks where the moving line is associated to the crack front and the obstacles are related to the microstructure of the material. The morphology of the fracture surface, which is the trace left behind by the propagating line, follows from the mor-

phology of the front at every instant. The existence of two regimes, characterized by two roughness exponents, is related to two different propagation modes. In the line models, the front is driven by an external force F. The external force has a threshold value below which the propagating line does not propagate and its average velocity is zero. For an external force equal to the threshold value, the line is able to propagate, freeing itself from the pinning obstacles but without acquiring a velocity. For external forces beyond the threshold value, the line propagates with a finite velocity. Close to the threshold, the moving line is self-affine with a roughness exponent or Hurst exponent H_c, characteristic of the so-called depinning transition. When a finite velocity appears, the quenched disorder term, characterizing in the motion equation the random but time-dependent character of the forces opposing the movement of the front, acts as noise. In this case the roughness of the interface can be characterized by a roughness exponent H, which is, *a priori* different H_c, at least beyond a characteristic length scale ξ_c. The crossover length between the H_c and H regimes decreases as the average velocity increases. When this velocity tends to zero, ζ_c diverges and the propagating line is at the depinning transition.

These theoretical predictions have been verified by E. Bouchaud et al. and Daguier et al.[33,34] in an Al alloy and glasses, respectively. In each case, the same two scaling regimes ($H_c = 0.5$ and $H = 0.78$) were observed. In both cases, the crossover length ξ_c separating these two regimes decreased with the average crack velocity. The decrease was similar for both materials (metal and glass), although three orders of magnitude separate the ξ_c for glass from those for the alloy having the same velocity. It can be noted that the two roughness exponents characterizing the fractal structure of the fracture surfaces are very close to our results. Bouchaud et al.[33] used advanced characterization techniques to study the origin of these two regimes. *In situ* observations of fractures showed that the propagating crack was preceded by nucleating and growing cavities. The crack was propagated by coalescence of existing cavities. This is indeed a very well-known fact in ductile fracture of metallic materials. In fact, the same ductile behavior has been observed in molecular dynamics simulations of ceramics and glasses, but at different length scales (atomic scale). Bouchaud et al. studied the cavities before they coalesced with the main crack. They found out that they exhibited a roughness exponent of 0.5 while the main crack and the cavities linked to it exhibited a roughness exponent of 0.8. This suggests two propagation modes: first, the nucleation and growth of cavities in front of the propagating crack, and then coalescence of the damage cavities. The change in roughness exponent from 0.5 to 0.8 occurring at the crossover length ξ_c suggests that ξ_c is the size of the cavities at coalescence. This is in agreement with the results of molecular dynamics simulations performed by Nakano et al.,[35] where the main crack was shown to progress by successive deflections at small length scales, while at larger length scales its propagation was due to an opening and coalescence of damage cavities. It is interesting to note that the same approach for modeling crack propagation, involving events happening at different length scales (and time scales) is used, for example, in geology to simulate fracture in rock material and to model earthquake faulting.[36–38]

These experimental results and numerical simulation predictions are in good agreement with our results. Our results suggest that, in the case of the copolymers, the first regime, at short length scales, was associated with the properties of the matrix, while the second regime at higher length scales was related to the presence of a second phase. The first regime, characterized by a low roughness exponent, can be understood in terms of cavities nucleating and developing in the matrix in front of the main crack. It seems then reasonable to believe that the first regime can be characteristic of the matrix. The second regime can be explained in terms of coalescence of damage cavities. The aim of the nodules or rubber particles introduced by the copolymerization is usually to stop the propagation of small cracks and to initiate new ones to increase the energy required for a fracture to propagate.

The maximum size of the small crack is then related in our case to the mean distance between nodules. This maximum size can be associated to ξ_c introduced earlier, to characterize the size of the cavities at coalescence. The propagation of the main crack is governed at length scales higher than ξ_c by the multiphase nature of he material while the nature of the small crack or cavities is governed by the nature of the matrix.

The fracture surface morphology is not the same everywhere. For example, shear lips, skin, and shear bands were observed on the fracture surfaces. The creation of these structures on the surface leads to energy dissipation, and the macroscopic behavior of the specimen is certainly related to the sizes of these structures relative to the fracture surface area. Only the morphology of the central part of the fracture surfaces was studied in detail, and this study should be extended to all the different regions in the fracture surfaces to obtain a more complete characterization of the surfaces and determine the influence of all regions on the toughness of the specimen. The sample geometry can be modified to minimize or increase the various components of the fractures surfaces. For example, it has been showed that shear lip formation can be avoided by working with side-grooved specimen.[39] It could then be possible to evaluate the influence of each part of the fracture surface on the macroscopic behavior and attempt to correlate the self-affinity of each of them with the energy dissipated during their formation.

CONCLUSIONS

The goal of this work was to study the structure of fracture surfaces to discover correlations between quantitative measures of the polymer structure and the mechanical properties of the final product. The surface structure can be described in terms of self-affine fractal models, and the Hurst exponent(s) and roughness measurements can be used to describe quantitatively the fracture surface topography. Fracture surfaces generated in homopolymers can be described by a single Hurst exponent, which differs for PE and PP. For copolymers with PE and PP matrices, the same Hurst exponent measured on small-length scales was the same as that obtained for the matrix material, but a crossover to a second regime characterized by a higher Hurst exponent was found at longer length scales. The crossover was related to the average distance between rubber particles for the PP/PE rubber phase specimen (PP-copo). A self-affine fractal behavior is not correlated with a two components composition, but it appears that the introduction of a second chemical entities modifies the crack propagation at long-length scales, the propagation at shorter length scales remaining unchanged. Environmental stress cracking experiments indicate that each regime can be related to brittle or ductile fracturing processes.

Our measurements have shown that a decrease in temperature leads to a decrease in rms roughness of 20% when it is measured over 1×0.5 mm areas and a lower fracture energy (except for HDPE-copo sample). At the same time, the Hurst exponent characterizing the self-affine structure of the fracture surfaces increases very slightly. This indicates that the fracture at 23°C are very similar to those generated at -20°C, even though the fracture energy changes a lot. The small variations in the rms roughness and the Hurst exponent values do not explain the observed changes in toughness. The fracture surfaces are very complex, and are composed of a central region and side regions (skin and shear bands, for example). It should be rewarding to studying the self-affine structure of each part individually (not only in the central part, which was the focus of our work), and try to correlate it the energy dissipated.

This work was supported by the Norwegian Research Council. The authors would like to thank Borealis for providing the samples and for use of their mechanical testing equipment. We would like to acknowledge Karstein Kleveland (Borealis AS) for encouraging and coordinating the collaboration with Borealis AS.

References

1. Lapique, F.; Meakin, P.; Feder, J.; Jøssang, T. J Appl Poly Sci 2000, 77, 2370.
2. Feder. J. Fractals; Plenum Press: New York, 1988.
3. Mandelbrot. B. B. The Fractal Geometry of Nature; Freeman: New York. 1983.
4. Mandelbrot, B. B.; Passoja, D. E.; Paullay, A. J. Fractal character of fracture surfaces of metals. Nature 1984, 308, 721.
5. Mitchell, M. W.; Bonner, D. A. J Mater Res 1990, 5, 2244.
6. Bouchaud, E.; Nave'os, S. J Phy 1995, 5, 547.
7. Friel, J. J.; Pande, C. S. J Mater Re 1993, 8, 100.
8. Lange, D. A.; Jennings, H. M.; Shah, S. P. J Am Ceram Soc 1993, 76, 589.
9. Mecholsky, J. J.; Passoja, D. E.; Feinberg-Ringe, K. S. J Am Ceram Soc 1989, 73, 60.
10. Brown, S. R.; Scholz, C. H. J Geophys Res 1985, 90, 12575.
11. Poon, C. Y.; Sayles, R. S,; Jones, T. A. J Phy D App Phys 1992, 25, 1269.
12. Schmittbuhl, J.; Roux, S.; Berthaud, Y. Europhy Lett 1999, 28, 585.
13. Schmittbuhl, J.; Schmitt, F.; Scholz, C. J Geophy Res 1998, 100, 5953.
14. Zhenyi, M.; Langford, S. C.; Dickinson, J. T.; Engelhatd, M. H.; Baer, D. R. J Mater Res 1991, 6, 183.
15. Engoy, T.; Maloy, K. J.; Hansen, A.; Roux, S. Phys Rev Lett 1994, 73, 834.
16. George Batrouni, G.; Hanson, A. Phys Rev Lett 1998, 80, 325.
17. Bouchaud, E.; Lapasset, G, Plan'es, J. Europhys Lett 1990, 13, 73.
18. Mecholsky, J. J.; Mackin, T. J. J Mater Sci Lett 1988, 7, 1145.
19. Schmittbuhl, J.; Vilotte, J. P. Phys Rev E 1995, 51, 131.
20. Bouchaud, E. J Phys Condens Matter 1999, 9, 4319.
21. Meakin, P. Scaling and Growth Far from Equilibrium. Cambridge University Press: Cambridge, 1998.
22. Lapique, F. Report Series from Cooperative Phenomena Project 97–2, Solid State Group, Institute of Physics, University of Oslo, 1997.
23. Mandelbrot, B. B. Phys Scr 1985, 32, 257.
24. Voss, R. F. In Scaling Phenomena in Disordered Systems; Pynn, R.; Skjeltorp, A., Eds.; NATO ASI Series B-133; Plenum Press: New York, 1985, p. 1.
25. Chui, C. F. An Introduction to Wavelets; Academic Press: Boston, 1992.
26. Simonsen, I.; Hansen, A.; Nes, O. M. Phys Rev E 1998, 58, 2779.
27. Goupillaud, P.; Grossmann, A.; Morlet, J. Geoexploration 1984, 23.
28. Arneodo, A.; Bacry, E.; Graves, P. V.; Muzy, J. F. Phys Rev Lett 1995, 74, 3293.
29. Arneodo, P.; d'Aubenton Carafa, Y.; Bacry, E.; Graves, P. V.; Muzy, J. F.; Thermes, C. Phys D 1996, 96, 291.
30. Leshorn, H. et al. Ann Phys 1997, 6, 1.
31. Bouchaud, J. P.; Bouchaud, E.; Lapasset, G., Planes, J. Phys Rev Lett 1993, 71, 2240.
32. Daguier, P.; Henaux, S.; Bouchaud, E.; Creuzet, F. Phys Rev E 1996, 53, 5637.
33. Bouchaud, E.; Paun, F. Comput Sci Eng 1999, 1(5), 32.
34. Daguier, P.; Nghiem, B.; Bouchaud, E.; Creuzet, F. Phys Rev Lett 1997, 78, 1062.
35. Nakano, A.; Kalia, R. K.; Vashishta, P. Phys Rev Lett 1995, 75, 3138.
36. Bobet, A.; Einstein, H. H. Int J Fract 1998, 92, 221.
37. Schmittbuhl, J.; Vilotte, J. P.; Roux, S. J Geophys Res 1996, 101, 27,741.
38. Silberschmidt, V. V. Pure Appl Geophys 2000, 157, 523.
39. Channel, A. D.; Clutton, E. Q.; Capaccio, G. Polymer 1994, 35, 3893.